

The Function of mRNA Decay in the Post-Diauxic Phase

A Thesis

Presented to


The Faculty of the Molecular Biology Department

The Colorado College

In Partial Fulfillment of the Requirements of the Degree

Bachelor of Arts


Primary Reader


Secondary Reader

By

Rachael Martino

April 2019

Abstract

Saccharomyces cerevisiae has the ability to alter its growth based on how much of a particular carbon source is present in the environment; when glucose is depleted the cells will enter the post-diauxic phase. Based on previous evidence, we suspect that mRNA that encode for mitochondrial proteins are degraded by a novel autophagic decay pathway in the post-diauxic phase, requiring the ribonucleases Xrn1 and Rny1 for proper mitochondrial growth. First, we tested the localization of the ribonucleases Xrn1 and Rny1 to determine if their localization changes due to stressful conditions, and if these results can indicate a change in their function. Second, to test if an autophagic mRNA decay pathway exists, we used the MS2 labeling technique to fluorescently tag specific mRNAs within the cell in order to see if they associate with structures that maybe involved in autophagic mRNA decay, such as autophagosomes and stress granules. We tested three specific mRNAs for their localization: *PGK1*, *DPI8* and *COX5A*. *PGK1* encodes for a protein kinase that aids in metabolism, while *DPI8* and *COX5A* both encode for mitochondrial proteins. We were able to determine that we can visualize mRNA using the MS2-CP-GFP fusion protein, however we believe that the MS2-CP-mCherry fusion did not detect MS2-tagged mRNAs. Using the MS2-CP-GFP assay, we were able to determine that *PGK1* localizes to mitochondria in the post-diauxic phase.

Introduction

***Saccharomyces cerevisiae* has Different Growth Conditions**

Saccharomyces cerevisiae is commonly known as bakers' yeast because it is the species of yeast that is used to make beer, bread, and wine. Not only does this yeast make delicious items, but *S. cerevisiae* is also a eukaryote, featuring a nucleus, mitochondria, and other membrane-bound organelles (Duina et al., 2014). *S. cerevisiae* has been one of the most studied model organisms because its genome was the first fully-sequenced eukaryotic genome and has helped in understanding many other eukaryotic species, specifically humans, with similar molecular characteristics (Goffeau et al., 1996). Many genes found in *S. cerevisiae* are similar to those that are found in humans, and with the ability to manipulate yeast's genome in the lab, we can easily use it to understand molecular mechanisms that are relevant to humans. One of the biggest advantages of using *S. cerevisiae* is its robust replicative power, where cells can replicate once every 90 minutes, providing a fast and easy way to accumulate a large number of cells in a short period of time.

S. cerevisiae cells have different growth phases that depend on the amount and type of nutrient source present (Wang et al., 1997). The first growth phase is the lag phase, which occurs right as the cells are placed in the nutrient-rich media. In this stage, the cells mature and become accustomed to the new conditions (Alsuheim et al., 2013). The next phase, the log phase, is a highly studied phase because the cells divide exponentially due to the high concentration of nutrients. Most organisms use anaerobic respiration in high glucose conditions; however, *S. cerevisiae* cells undergo fermentation using glucose as their fuel source and producing ethanol as a byproduct, which is then used as the main energy source for the

next phase. The metabolic switch from fermentation to respiration is called the diauxic shift, which is the point between the log and post-diauxic phase (DeRisi et al., 1997). The post-diauxic phase occurs once glucose has been depleted, causing the rate of growth to slow. Due to the abundance of ethanol produced in the log phase, the cells in the post-diauxic phase perform respiration to break down ethanol for energy. The stationary phase is the fourth and final growth phase. It occurs when most of the nutrient sources, such as carbon and nitrogen, are depleted, thus halting cell growth. Overall, cells in a variety of organisms will fluctuate between nutrient-poor and nutrient-rich conditions on a daily basis, which requires altering which genes are expressed to allow for the cells to adapt.

The Post-Diauxic Phase in *S. cerevisiae*

The post-diauxic growth phase is generally understudied, but it is of extreme interest because it can give us a mechanistic insight into how eukaryotic cells survive during stressful conditions and how they adapt to changing environmental conditions to maintain homeostasis. In the post-diauxic phase, cells change their main carbon source from glucose to ethanol, allowing the cells to adapt to use the ethanol as an energy source (an energy poor 2 carbon alcohol). Due to this metabolic change, the cell has to shift many cellular functions in order to maintain homeostasis. This metabolic stress is similar to stressful conditions that human muscle cells endure (Otterstedt et al., 2004). Glucose is one of the main energy sources for human muscle cells. However, during high intensity exercise, oxygen cannot get to the cells in time to produce ATP through aerobic respiration. Therefore, in order to make ATP, the human muscle cells must alter their cellular functions to utilize the glucose through fermentation, producing lactic acid. Similar to *S. cerevisiae*, human cells have to alter their functions in order to respire

ethanol. To achieve this cellular change, it has been observed that the diauxic-shift is correlated with a widespread change in gene expression, such as a significant decrease in transcription and translation levels (DeRisi et al., 1997).

Changes in Gene Expression that Occur in the Post-Diauxic Phase

Maintaining homeostasis is a key part in cell survival, especially during stressful conditions similar to those experienced in the post-diauxic phase. This can be achieved by altering transcription, translation, and autophagy to adjust the expression profile to match the needs of the cell. It has been observed that levels of transcription are lower after the diauxic-shift and are three to five times lower approaching the stationary phase compared to the log phase (Galdieri et al., 2010). Also, at the diauxic-shift, it has been identified that translational apparatus and ribosomal proteins are strongly repressed in *S. cerevisiae* (Stahl et al., 2004). This shows that cells may adapt by dramatically decreasing levels of transcription and translation in the post-diauxic phase. It was also observed that significant changes to the mRNA expression are observed between the log phase and the post-diauxic phase. For example, the mRNA levels of approximately 1,030 genes declined by a factor of 2, while 710 genes increased by a factor of 2 (DeRisi et al., 1997). mRNA that encode for pyruvate decarboxylase was observed to be downregulated at the diauxic shift because it is an enzyme that aids in the production of ethanol during fermentation in *S. cerevisiae* and is not needed in the post-diauxic phase. This regulation is pivotal to the cell because at the diauxic shift, fermentation can no longer occur, and respiration takes over to produce energy. On the other hand, it was observed that the mRNA that encode for mitochondrial ribosomal genes were induced, exemplifying the importance of mitochondrial function in the post-diauxic phase (DeRisi et al., 1997). These

examples further the point that the cell must alter its normal functions in order to maintain homeostasis and suggest that the regulation of mitochondria is very important for the post-diauxic phase.

Mitochondria is a key organelle in all eukaryotes because it is the largest energy producer in the cell. In yeast, when glucose is not present, mitochondria are essential for the cell to process ethanol to produce energy through cellular respiration, and hence are important for yeast to grow in the post-diauxic phase. Without functioning mitochondria, the yeast would not be able to produce energy from ethanol and could no longer divide. The same goes for human cells. Without mitochondria, the human body would not be able to function because the mitochondrial inner membrane is where most of the ATP is synthesized. Mitochondria are very unique organelles in that the genes that are required for their function are encoded in the nuclear genome as well as their own circular genomes found within themselves. Interestingly, it has been observed that some of the nuclear encoded mRNAs necessary for mitochondrial function are translated on the surface of the mitochondria to aid in the quick translation and localization of mitochondrial proteins (García-Rodríguez et al., 2007). Overall, mitochondria are one of the most important organelles because without mitochondria, there could be damaging effects on the cell or organism. For example, defects in respiration and proper mitochondrial function have correlated with neurodegenerative diseases, such as Alzheimer's disease, where the abrogation of autophagy to rid the cell of defective mitochondria is correlated with the disease (Alirezai et al., 2010).

Autophagy is an important process for cell survival because it regulates and discards any component that is either unwanted, not needed, or dysfunctional in the cell, especially during

stress like in the post-diauxic phase. It has also been observed that autophagy levels increase during the post-diauxic phase due to the accumulation of glycogen and other storage molecules (Noda and Ohsumi, 1998), leading to an increase in protein degradation and thus a decrease in gene expression. For autophagy to occur, the cell will first receive a starvation signal and mark substrates post-translationally to undergo autophagy. Once the cell has received this signal, a double membrane layer will form around the marked substrate, forming an autophagosome (Klionsky and Emr, 2017). The autophagosome will then travel and fuse with the vacuole, losing one of the outer membranes. Once in the vacuole a vacuolar lipase, Atg15 will degrade the second outer membrane so digestive enzymes, such as proteases, can then degrade the contents inside the fused autophagosome (Welter et al., 2014). Autophagy can target many different cellular components for degradation, such as ribosomes, through a process called Ribophagy. Ribophagy is a well-known degradation pathway in *S. cerevisiae* and mammalian cells, and ribosomes have been found to be highly targeted for autophagy in starvation conditions (Cebollero et al., 2011). Additionally, stress granules undergo autophagy in the post-diauxic phase. Stress granules are messenger ribonucleoprotein complexes (mRNPs) that contain mRNA that is translationally repressed, and form when translation initiation is halted (Buchan et al., 2013). Therefore, in the post-diauxic phase when translation levels are low, mRNA will accumulate and form stress granules. Finally, just like stress granules, mitochondria undergo autophagy through a process called mitophagy, which occurs in both yeast and human cells (Youle and Narendra, 2011). This is an imperative process because damaged mitochondria produce free radicals that can cause damage to the cell. The mitochondria need to be removed from the cell as to prevent DNA mutations and other damage that can be caused by the highly-

reactive free radicals. Damaged mitochondria, stress granules, ribosomes, and P-Bodies all undergo autophagy, and we believe that the RNA or mRNA associated with each undergo decay in the vacuole. Thus, it is possible that autophagy may also degrade RNA to alter gene expression during the post-diauxic phase. It is well known that the standard functions of translation, transcription, and autophagy change to alter gene expression in the post-diauxic phase to maintain homeostasis, but how mRNA decay changes remain unknown in the post-diauxic phase.

The Roles of Autophagy and mRNA Decay in Regulating Gene Expression

A key factor connecting autophagy and mRNA decay is Rny1. Rny1 is the only T₂ RNase present in *S. cerevisiae*, however, it is highly conserved in humans. Rny1 has been observed to be upregulated during stressful conditions (MacIntosh et al., 2000). Other experiments performed on Rny1 determined that it is required for the cleavage of tRNA and rRNA molecules in the cell in stressful conditions (Luhtala et al., 2012). It is unknown if Rny1 leaves the vacuole in order to cleave these molecules, or if the tRNAs and rRNAs travel to the vacuole. Luhtala et al determined that there was a decrease in vacuolar signal for the Rny1-GFP strain during oxidative stress. This could suggest that in stressful conditions, Rny1 will exit the vacuole to the cytoplasm to aid in the cleavage of tRNAs and rRNAs.

To further understand this possible connection between mRNA degradation and autophagy, our lab looked into the effect of mRNA decay and autophagy using RNA-Sequencing. When the Rny1 gene was deleted from the genome, there was an upregulation of 814 different mRNAs in the post-diauxic phase. We also observed that 392 mRNAs were upregulated when Atg15 was deleted (Figure 1a). Of those, 187 of the mRNAs that were

upregulated in both Rny1 and Atg15 were individual deletions. This suggests that those 187 mRNAs are likely targets for autophagic mRNA decay by Rny1. Interestingly, approximately 40% of the 187 mRNAs encode for mitochondrial proteins (Figure 1b). It is well known that RNA undergo decay by ribonucleases such as Rny1, however, we believe that autophagy may represent another mRNA decay pathway in the post-diauxic phase.

Generally, mRNA decay is regulated by ribonucleases in different parts of the cell and is viewed as a key part of gene expression as it provides a very fast mechanism to alter mRNA levels based on the conditions which the cell encounters. Xrn1 is one of the main exonucleases in the cell because it serves to degrade a wide variety of mRNAs and is expressed at very high levels (Grousl et al., 2015). Xrn1 degrades mRNA 5' to 3' once the 5' protective cap and 3' polyadenylated tail have been removed (Grousl et al., 2015). Xrn1 is localized mostly to the cytoplasm of the cell in the exponential log phase, but it has been observed that Xrn1 will also associate with P-Bodies in the log phase and post-diauxic phase. P-Bodies are ribonucleoprotein assemblies and can be found in unstressed cells, but are formed at a higher rate when the cell is under stressful conditions, such as glucose deprivation. Xrn1 localizes to P-Bodies along with all of the mRNA degradation machinery needed to aid in this process, such as decapping enzymes and degradation activators. The localization of Xrn1 to P-Bodies has been viewed as a region where Xrn1 is active and will be capable of degrading unstable mRNAs, as it is one of the main exonucleases in *S. cerevisiae*. However, once the cells enter the post-diauxic phase, Grousl et al suggests that Xrn1 has been shown to localize away from P-Bodies and therefore may change its function in the post-diauxic phase.

Xrn1 and Rny1 may both be required for proper function in the post-diauxic phase. When both of the genes that encode for Xrn1 and Rny1 were deleted from the genome, these strains showed phenotypes that indicated that they lacked properly functioning mitochondria. First, *rny1Δxrn1Δ* mutants grew as petite colonies (Figure 2). Petite colonies signify that the cells did not have functioning mitochondria as their growth was stunted and had a white phenotype as respiration did not occur in these cells. Also, when *rny1Δxrn1Δ* mutants were grown on glycerol containing media, there was very little growth (Figure 3b) compared to the double mutant grown on normal media containing glucose (Figure 3a). In order for a cell to grow on glycerol media, the cell must respire, thus mitochondria must be functioning. Furthermore, *rny1Δxrn1Δ* cells were stained with a dye that stains active mitochondria called Mitotracker, and there were little to no mitochondria staining present in these cells (Figure 3c). These experiments support that Xrn1 and Rny1 work in parallel pathways to create or promote functional mitochondria and illustrate that RNA degradation is important for the survival of the cell in nutrient-limiting conditions, such as the post-diauxic phase.

Understanding the Role of mRNA Decay During the Post-Diauxic Phase

mRNA decay and mitochondrial function are both imperative processes for cell function and maintaining homeostasis. Therefore, our central question for our research is two-fold; how does mRNA decay affect mitochondrial function, and how does mRNA decay promote proper gene expression in the post-diauxic phase. Autophagy could be a key factor in both parts of our research question as the mRNAs that are translated on the surface of the mitochondria could also be degraded by autophagy. We also hypothesize that mRNAs that associate with stress granules that also undergo autophagy may be subject to a similar fate. Finally, we understand

how the levels of transcription and translation fluctuate during the post-diauxic phase, but it is unknown the contribution that mRNA decay may play in conditions of stress.

To address these questions, first we wanted to characterize the function of Xrn1 and Rny1 in the post-diauxic phase through their localization. Second, we tested if an autophagic mRNA decay pathway does exist using the MS2 system to determine the localization of specific mRNAs that may undergo autophagic mRNA decay. We were able to determine that Xrn1 did localize to P-Bodies and Rny1 localized to mitochondrial-like structures in the post-diauxic phase. This signifies that Xrn1 stays within P-Bodies in the post-diauxic phase and will continue to degrade its specific subset of mRNAs there. On the other hand, Rny1's localization suggests that it localizes near or within mitochondrial-like structures. This coincides with our hypothesis that Rny1 aids in maintaining mitochondria function as it is localized close to the mitochondria and can work closely with them.

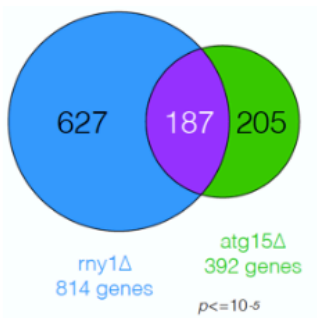
Using the MS2 System to Determine the Localization of mRNAs in a Live Cell

From our previous research, we were able to form a hypothesis that Xrn1 and Rny1 work in parallel pathways to create functioning mitochondria and that Rny1 and autophagy may be involved in a novel mRNA decay pathway. From the previous RNA-Sequencing experiments performed, we deduced that *DPI8* and *COX5A* mRNA levels increase when Rny1 and autophagy function is impaired, while *PGK1* mRNAs do not change and could be used as a control mRNA. To test our hypothesis that Rny1 may mediate an autophagic mRNA decay pathway, we decided to look at the colocalization between these specific mRNAs and mitochondria, stress granules, and autophagosomes. If our mRNAs do in fact colocalize with the latter two structures, then this may suggest they may undergo autophagic mRNA decay.

To do this, we generated strains that had specific mRNAs tagged with MS2 stem loops (Figure 4). In these strains, we expressed an MS2 coat protein fused to a fluorescent protein that was bound to the MS2 stem loops within the specific mRNA allowing for its visualization. This MS2 system allowed us to visualize specifically where mRNA is localized in a living cell (Tutucci et al., 2018). Next, we introduced components of stress granules and autophagosomes that have been tagged with GFP or mitochondria that have been tagged with mCherry to visualize each of the structures *in vivo*. We were able to determine that our MS2-CP-GFP fusion protein was successful in visualizing mRNA in a live cell and from this strain we were able to deduce that *PGK1* localizes to mitochondria in the post-diauxic phase.

Figures

A



B

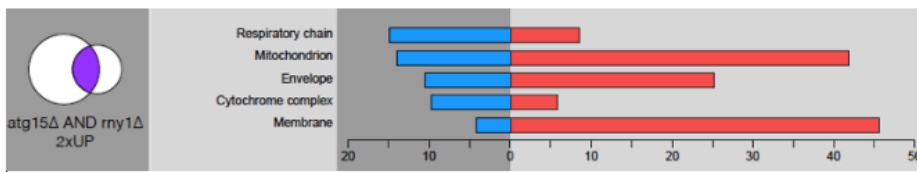


Figure 1: Mitochondrial mRNAs are upregulated in *atg15Δ* and *rny1Δ* strains. (A) Rny1 and Atg15 were each deleted from the WT strain and the mRNA levels were measured by RNA-seq in the post-diauxic phase. (B) mRNAs that encode for mitochondrial proteins are upregulated in *rny1Δ* and *atg15Δ* compared to WT. Mitochondrial mRNAs were found to be upregulated in the double deletion strain. Blue: significance, Red: cluster frequency, percent of RNAs that have that specific go-term.

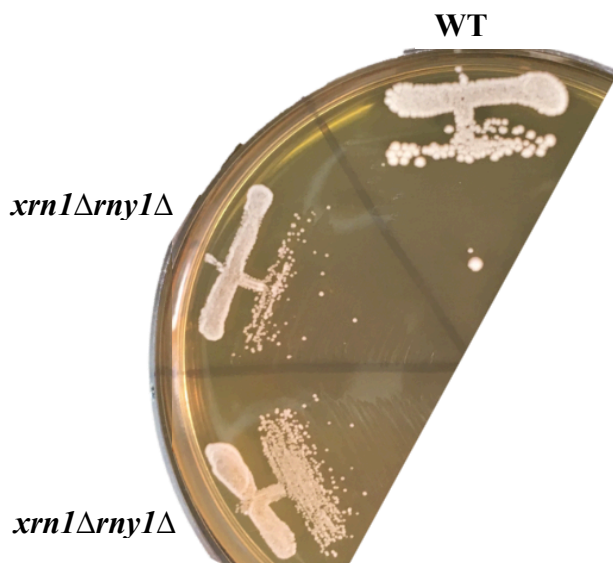
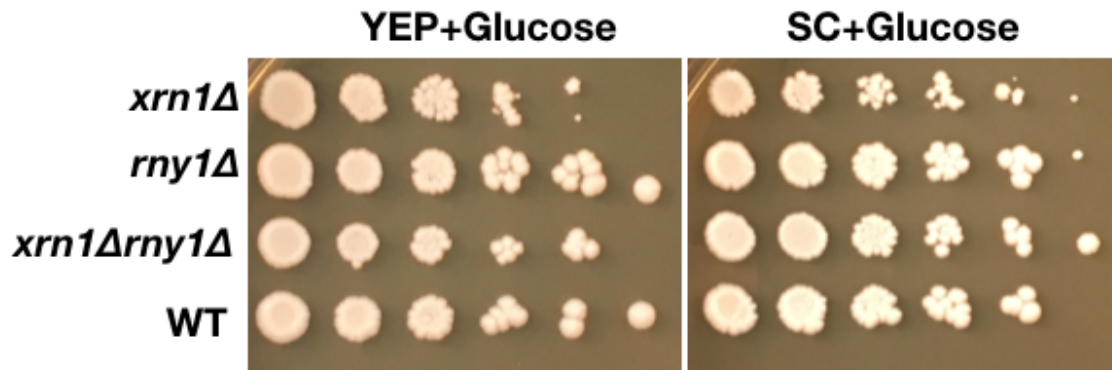
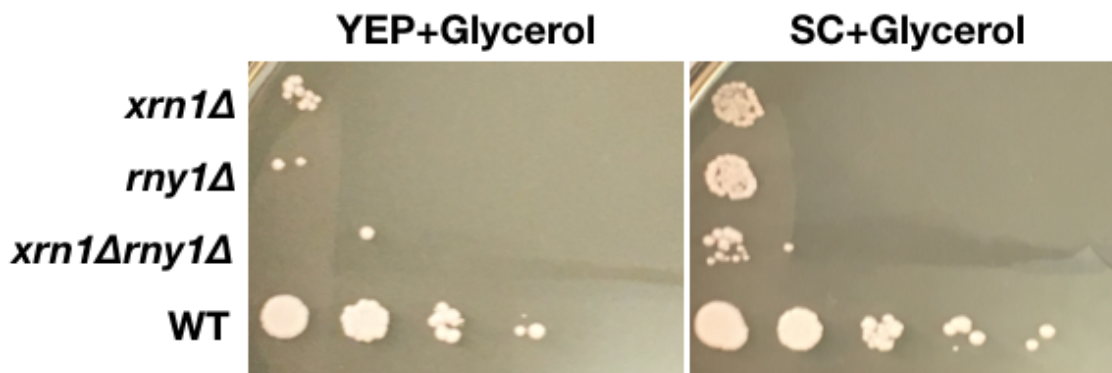


Figure 2: Petite colonies were observed when Xrn1 and Rny1 were deleted. Xrn1 and Rny1 were both deleted creating the *xrn1Δrny1Δ* mutants and were streaked out along with WT. Petite colonies were observed.

A



B



C

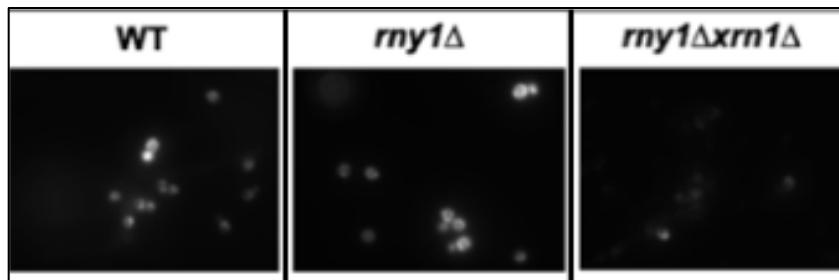


Figure 3: *xrn1Δrny1Δ* cannot grow on media with glycerol and do not have functioning mitochondria (A) Xrn1 and Rny1 were each individually deleted from the WT strain or from an *xrn1Δ* strain by transformation. All three strains, plus WT were grown on YEP + glucose media and SC + glucose media. (B) The same four strains were grown on YEP + glycerol media and SC + glycerol media. (C) Mitochondria was stained using Mitotracker and observed in WT, *rny1Δ* or *rny1Δxrn1Δ* strains. All stained strains were visualized using a fluorescence microscope.

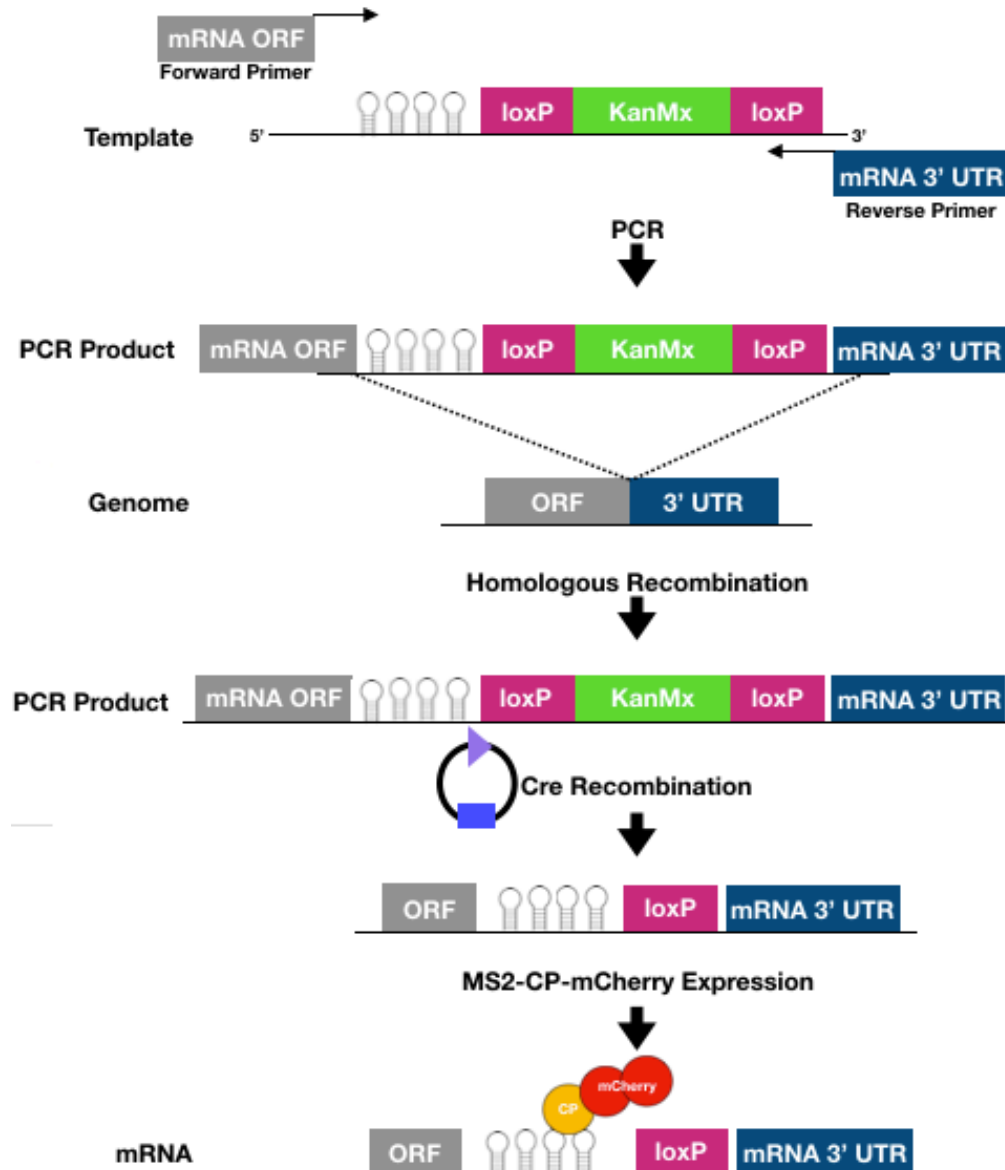


Figure 4: Tagging *PGK1*, *DPI8* and *COX5A* with MS2. Schematic of how three different mRNAs; *PGK1*, *DPI8*, and *COX5A*, were all tagged with MS2 to allow for the visualization of the RNA using mCherry or GFP MS2 fusion proteins using the MS2 system. mRNA primers were designed with 50 base pairs of homology from *PGK1*, *DPI8*, or *COX5A* to amplify the template DNA. A PCR was performed giving the PCR product that was then, through transformation and with homologous recombination, inserted into the genome. Next, the Cre-Recombinase plasmid was transformed into the cells and induced, removing the KanMx antibiotic resistant marker. Finally, GFP or mCherry was transformed into the cell and was fused to the RNA stem loops.

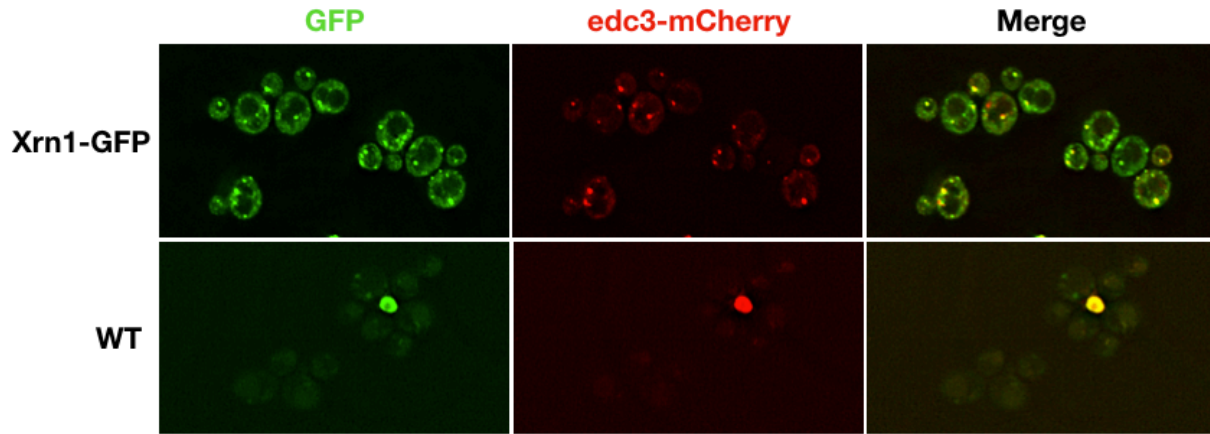


Figure 5: Xrn1 colocalizes with P-Bodies in the post-diauxic phase. Xrn1 was tagged with GFP and P-Bodies were visualized by expressing EDC3-mCherry. Wild-type cells were also visualized using the same conditions as the Xrn1-GFP to control for autofluorescence. The cells were back diluted in SC-URA media containing 2% glucose to an $OD_{600} \sim 0.2$ and grown at 30°C for 20 hours. The cells were then placed on a 1% agar pad and visualized under the microscope.

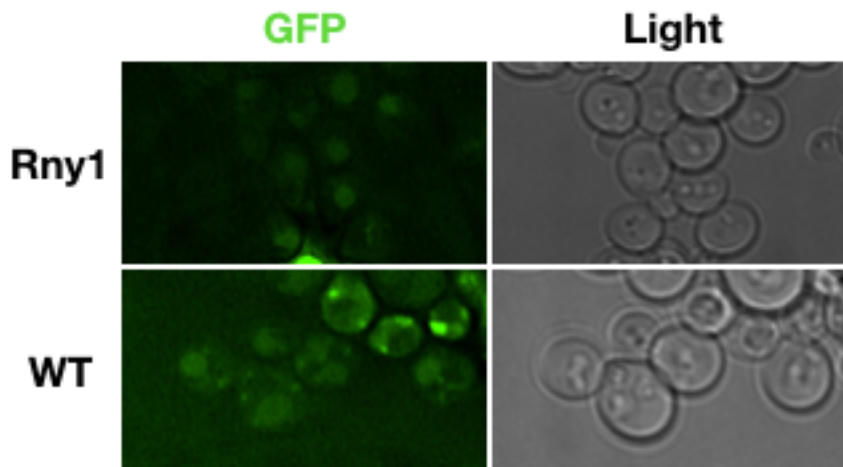


Figure 6: Rny1 is not detected in the log phase. Rny1 was internally tagged with GFP. The cells were back diluted in SC media containing 2% glucose to an $OD_{600} \sim 0.2$ and grown at 30°C for 3.5 hours to an $OD_{600} \sim 0.5$. The cells were then placed on a 1% agar pad and visualized under the microscope.

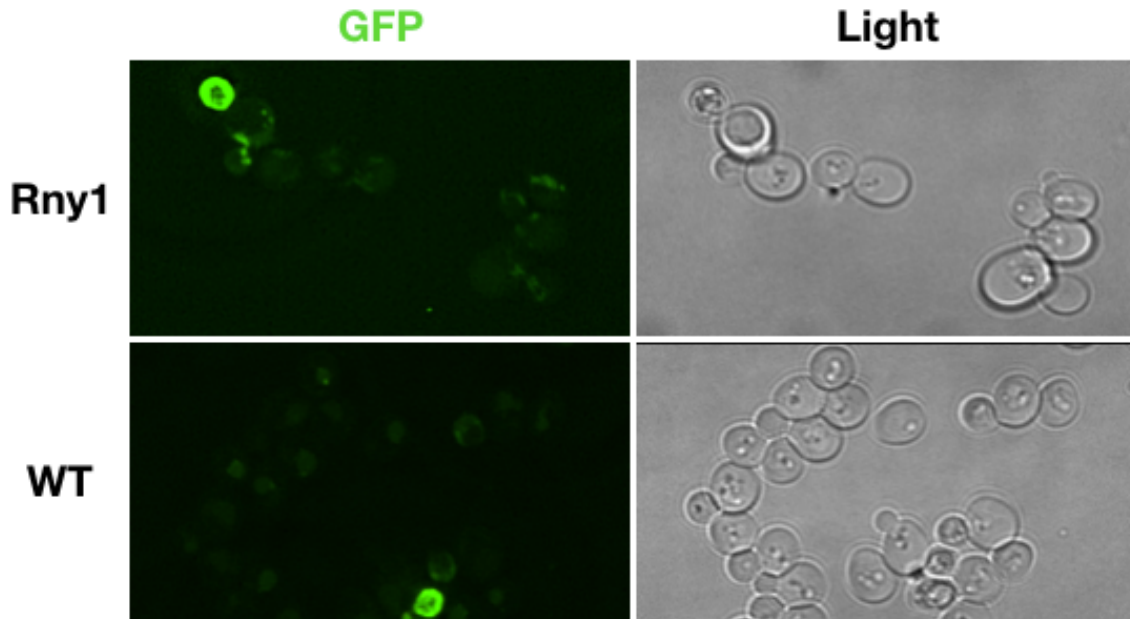


Figure 7: Rny1 localizes with mitochondria in the post-diauxic phase. Rny1 was internally tagged with GFP. The cells were back diluted in SC media containing 2% glucose to an $OD_{600} \sim 0.2$ and grown at 30°C for 20 hours. The cells were then placed on a 1% agar pad and visualized under the microscope.

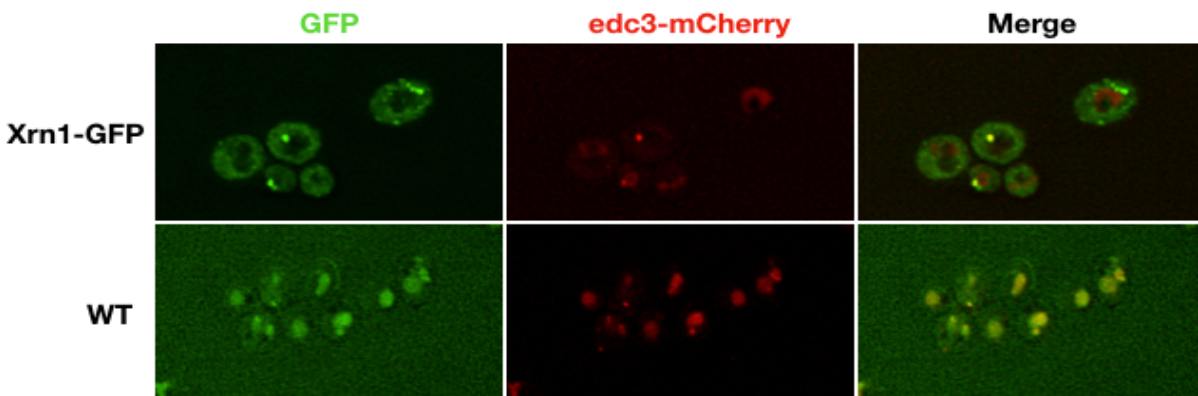


Figure 8: P-bodies are localized to the vacuole in ethanol media. Xrn1 was tagged with GFP and P-Bodies were tagged with edc3-mCherry. Wild-type cells were also visualized using the same conditions as the Xrn1-GFP to control for autofluorescence. The cells were back diluted in SC media with 3% ethanol to an $OD_{600} \sim 0.2$ and grown at 30°C for 20 hours. The cells were then placed on a 1% agar pad and visualized under the microscope.

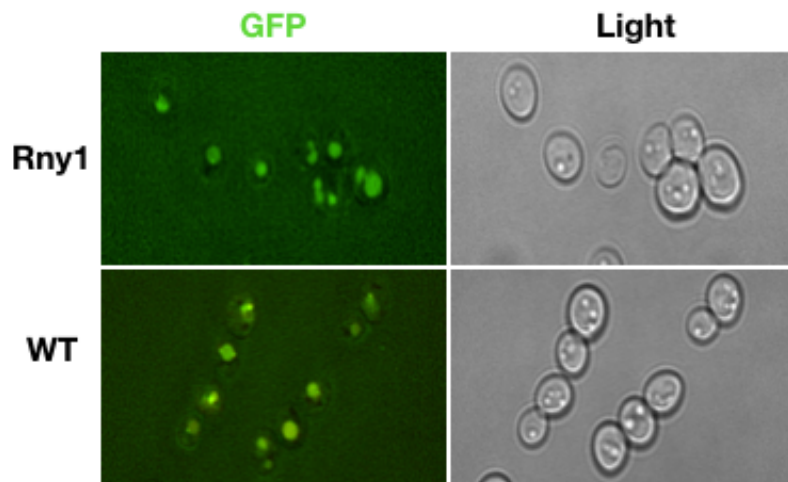


Figure 9: Rny1 is not visualized in cells grown in ethanol media. Rny1 was internally tagged with GFP. Wild-type cells were also visualized using the same conditions as the Rny1-GFP to control for autofluorescence. The cells were back diluted in SC media with 3% ethanol to an $OD_{600} \sim 0.2$ and grown at 30°C for 20 hours. The cells were then placed on a 1% agar pad and visualized under the microscope.

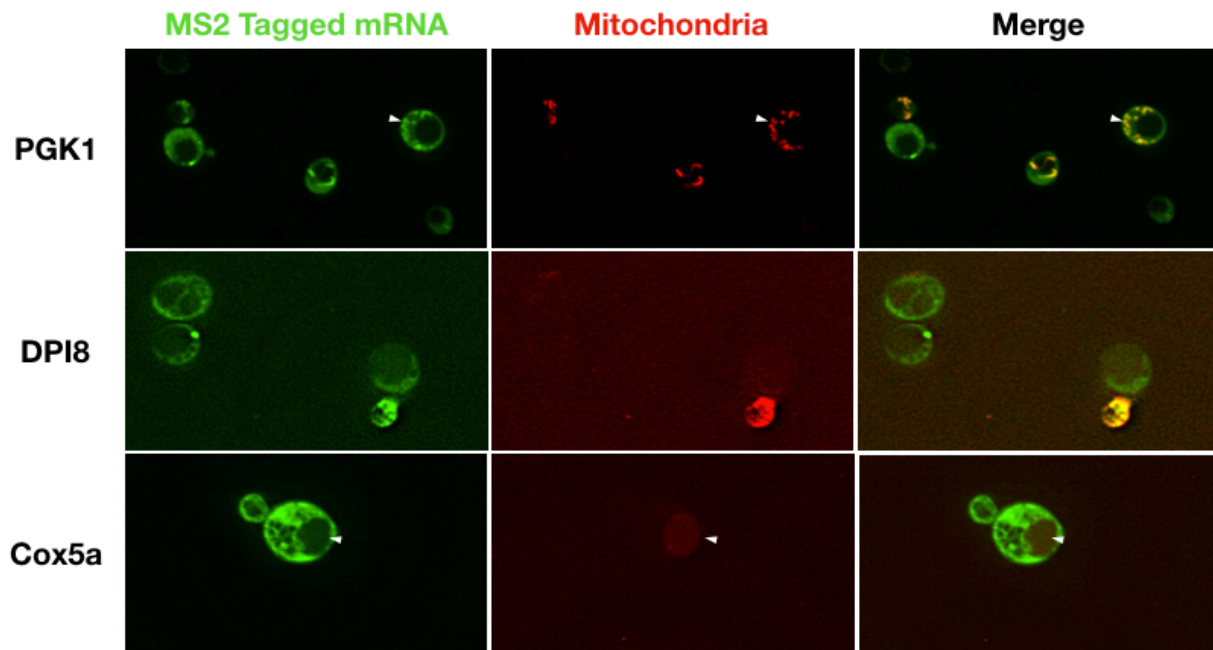


Figure 10: mRNA and mitochondria localization in the post-diauxic phase. *PGK1*, *DPI8*, and *COX5A* mRNAs were all tagged with GFP and mitochondria were tagged with mCherry. The cells were back diluted in SC-URA-HIS media with selective amino acids to an $OD_{600} \sim 0.2$ and grown at 30°C for 20 hours. The cells were then placed on a 1% agar pad and visualized under the microscope.

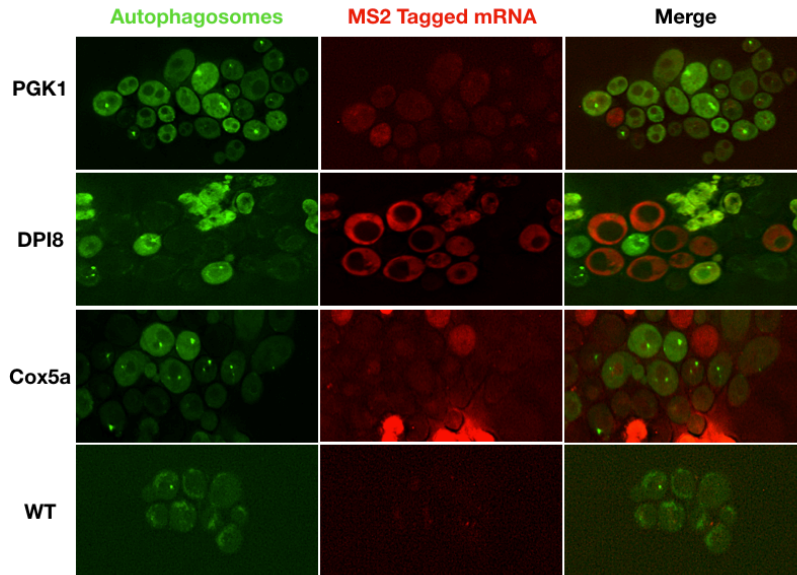


Figure 11: mRNA and autophagosome localization in the post-diauxic phase. All three mRNAs were tagged with mCherry using MS2 and autophagosomes were tagged with GFP by expressing GFP-ATG8. The cells were back diluted in SC-LEU-HIS media to an $OD_{600} \sim 0.2$ and grown at 30°C for 20 hours. The cells were then placed on a 1% agar pad and visualized under the microscope.

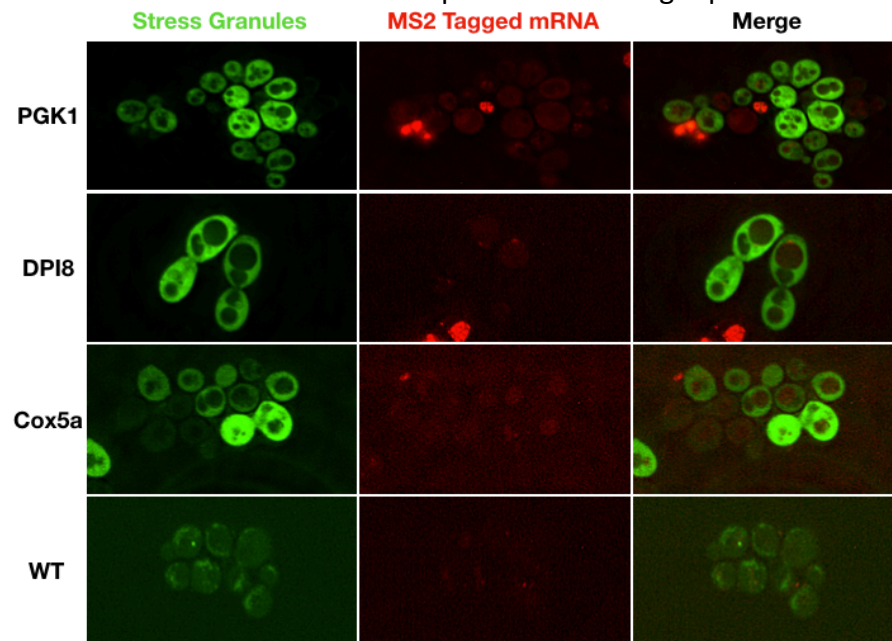


Figure 12: mRNA and stress granule localization in the post-diauxic phase. All three mRNAs were tagged with mCherry using MS and stress granules were tagged with GFP by expressing Pab1-GFP. The cells were back diluted in SC-HIS-LEU media with selective amino acids to an $OD_{600} \sim 0.2$ and grown at 30°C for 20 hours. The cells were then placed on a 1% agar pad and visualized under the microscope.

Results

Xrn1 Localizes to P-Bodies in the Post-Diauxic Phase

As one of the main ribonucleases in *S. cerevisiae*, we were curious to observe the localization of Xrn1 in the different growth phases because it was previously observed to alter its localization, which in theory could change its function in the post-diauxic phase. It is well known that Xrn1 is localized to the cytoplasm in nutrient-rich conditions, but a recent study suggested that the localization of Xrn1 in the post-diauxic phase is within eisosomes at the cell membrane (Grousl et al., 2015). We sought to repeat this result for ourselves as it would suggest that the function of Xrn1 would change during the post-diauxic phase.

To replicate these results, Xrn1 was tagged with GFP and P-Bodies were visualized by expressing Edc3-mCherry. The cells were grown in a minimal SC media containing 2% glucose, back-diluted to an OD of approximately 0.2 and grown for 20 hours at 30°C. At 20 hours, the cells had entered the post-diauxic phase as they had consumed the limited amount of glucose present. Xrn1-GFP appeared throughout the cell as well as localized into bright cytoplasmic green foci (Figure 5). This result indicates that Xrn1 does in fact colocalize with P-Bodies during the post-diauxic phase as we observed Xrn1-GFP within Edc3-mCherry marked P-Bodies. This is apparent for many of the foci that were identified (Figure 5). We were not able to replicate the results from Grousl et al, but we can clearly see that Xrn1 remains in the cytoplasm, colocalized with P-Bodies in the post-diauxic phase.

Rny1 Localizes to Mitochondria-like Structures in the Post-Diauxic Phase

The localization for Rny1 has always been dubious. Rny1 has been suggested to localize to the vacuole to aid in ribophagy and bulk RNA autophagy during stressful conditions (Welter et al., 2014). On the contrary, Rny1 has also been observed to leave the vacuole to the

cytoplasm to degrade tRNAs and rRNAs in stressful conditions (Thompson et al., 2009, Luhtala et al., 2012). Therefore, we wanted to determine the exact localization of Rny1 in the post-diauxic phase. We hypothesized that Rny1 is not expressed or active until the post-diauxic phase because we performed RNA-sequencing experiments with a *rny1Δ* strain grown either to the log phase or the post-diauxic phase. There was no real effect on mRNA levels when Rny1 was deleted from the genome in nutrient-rich conditions (data not shown), however there was an increase in 1,064 mRNAs in the post-diauxic phase.

We generated an internally-tagged Rny1-GFP by CRISPR to visualize Rny1 in both log and post-diauxic cells. In the log phase, we were not able to detect Rny1-GFP because of strong autofluorescence of the vacuole in both the Rny1-GFP strain and the untagged WT strain (Figure 6). Therefore, we could not determine where Rny1-GFP localizes in the log phase. However, we were able to visualize Rny1-GFP in the post-diauxic phase. The Rny1-GFP cells were grown to the post-diauxic phase, and Rny1 was not found in the vacuole in the post-diauxic phase. However, it looked to be localized to mitochondria-like structures in the cytoplasm (Figure 7) as mitochondria localization appears in the cytoplasm and is typically long and non-uniform in shape. This is the shape that Rny1 appears to be in Figure 7.

P-bodies are Localized to the Vacuole when Growth in 3% Ethanol Media

Since the main carbon source for cells in the post-diauxic phase is ethanol, we tested to see how the localization of Xrn1 and Rny1 would change if we grew the cells in 3% ethanol media. Ethanol containing media should similarly emulate the post-diauxic phase because ethanol is the main carbon source used by the cells. However, if we place cells grown to the log phase in the ethanol media, it would place the exponentially dividing cells in an immediately

stressful condition as the cells have not prepared or altered any of their gene expression patterns to deal with the stress of changing carbon sources. When log phase cells expressing Xrn1-GFP and the P-Body protein, Edc3-mCherry, were placed into 3% ethanol media and grown for 20 hours, we were able to see that P-Bodies changed their localization relative to Xrn1-GFP. Edc3-mCherry marked P-Bodies are normally found in the cytoplasm in the post-diauxic phase (Figure 5), but in ethanol media, they appeared to be localized to the vacuole (Figure 8). On the other hand, Rny1-GFP signal was not detected in ethanol media as the Rny1-GFP and WT strain both had autofluorescence in the vacuole, making it difficult to distinguish where Rny1-GFP is localized to in ethanol media (Figure 9). Our findings suggest that when the cells are immediately placed in a stressful condition and allowed to grow, P-Bodies will no longer co-localize with Xrn1, and thus, may alter Xrn1 activity.

mRNA Visualization in the Cell using the MS2 system

After we determined potential targets of mRNA decay by autophagy through RNA-seq experiments with Rny1 and Atg15 deletions in the post-diauxic phase, we wanted to observe the localization of these mRNAs in the cell during this phase. If we are able to determine where these mRNAs are located in a live cell in the post-diauxic phase, then it can provide insight into the how these mRNAs are regulated. We chose to tag *PGK1* as a negative control mRNA because the level of expression of *PGK1* did not change when we deleted Rny1 in the post-diauxic phase, while *DPI8* and *COX5A* mRNAs increased by two-fold or more when either Rny1 and Atg15 were deleted. We hypothesized that *DPI8* and *COX5A* would localize with stress granules, autophagosomes, and/or mitochondria, while *PGK1* would only localize with mitochondria as we predict that *DPI8* and *COX5A* would undergo autophagic mRNA decay while

PGK1 would not. To visualize mRNA in a live cell, we created MS2 tagged mRNAs by first creating a PCR product that contained MS2-RNA stem loops that can be targeted to insert into our gene of interest. These PCR constructs were then transformed and integrated into the genome after the stop codon of each gene that we chose to analyze its mRNA localization. After the construct containing the MS2 stem loops was properly targeted, the selectable marker was removed using Cre-recombinase, leaving a gene that encoded an mRNA that contained with the MS2-stem loops. These MS2-stem loops allow for the binding of the MS2 Coat Protein, fused with either the red or green fluorescent protein (MS2-CP-GFP or MS2-CP-DsRed), and the visualization of the MS2-tagged mRNA (Figure 4) allowed us to track the MS2-tagged mRNA using an epifluorescence microscope. In order to determine if the mRNAs are in fact localized with these various cellular components, we first must see if we can visualize the mRNAs and see that our fluorescent proteins that tag stress granules, autophagosomes, and mitochondria can be visualized properly.

***PGK1* Colocalizes with Mitochondria, but *COX5A* and *DPI8* do not**

PGK1 is an mRNA that encodes for a protein that localizes to the mitochondria, but its levels did not increase in the post-diauxic when Rny1 or Atg15 was removed. Therefore, we believe that *PGK1*-MS2-tagged mRNA should not colocalize with stress granules or autophagosomes as it should not be subjected to autophagic mRNA decay, but rather it should localize to mitochondria. As expected, we found that *PGK1*-MS2-tagged mRNA colocalized with mitochondria (Figure 10). We predicted this result because *PGK1* encodes for proteins that create kinases that will participate in glycolysis, and it was previously identified that *PGK1* protein is localized to the mitochondria (SGD). To our surprise, neither *DPI8*-MS2-tagged mRNA

nor COX5A-MS2-tagged mRNA looked like they localized with mitochondria as both of these mRNAs encoded for mitochondrial proteins (Figure 10). It seems like in these strains, the mitochondria are not apparent as the cells lacked observable long and stringy red fluorescent structures. We are unsure as to why the mitochondria were not observed in these strains. This could be due to a technical error, such as the loss of the plasmid expressing the red mitochondrial marker, pMito-DsRed, or the MS2-tag is somehow compromising mitochondria. Interestingly, we saw that the COX5A-MS2 tagged strain had Mito-dsRed red fluorescence in the vacuole in the post-diauxic phase (Figure 10). It is possible that the mitochondria may be in the vacuole in these strains. We know that mitochondria undergo autophagy (Youle and Narendra, 2011), however, the insertion of the MS2 cassette could alter the RNA to render mitochondria defective in this strain, and therefore we cannot conclude much. Both the DPI8-MS2 tagged and COX5A-MS2 tagged mRNA showed fluorescence signal in the cytoplasm of the cell, but since we were unable to visualize mitochondria in these strains, we could not conclude the localization of these mRNAs in the post-diauxic phase.

The MS2-CP-DsRED Signal did Not Work but Autophagosomes were Successfully Visualized

Next, we tested if we can observe the fluorescence of a set of strains that contained the MS2-tagged mRNAs visualized by an MS2 coat protein tagged with DsRed and autophagosomes tagged with GFP. If we can observe these tags, we can test if these mRNAs colocalize with autophagosomes because this may suggest that the mRNA does in fact undergo autophagic mRNA decay. In all three strains, we are able to visualize autophagosomes as strong circular GFP foci in each cell (Figure 11). We can see that PGK1-MS2 tagged mRNA is localized throughout cytoplasm of the cell, without any obvious foci. This result is different than what we

saw previously in Figure 10 because MS2-CP-DsRed signal in the PGK1-MS2 tagged strain was not localized to mitochondria like we observed in the PGK1-MS2-tagged strain using the MS2-CP-GFP fusion protein. This led us to believe that there was a problem with the MS2-CP-DsRed plasmid in this strain and what we are seeing is not the true localization of the PGK1-MS2 mRNA. Therefore, we cannot say if the *PGK1* mRNA associates with autophagosomes in these strains expressing MS2-CP-DsRed. Again, we hypothesized that DPI8-MS2-tagged and COX5A-MS2-tagged mRNA would colocalize with autophagosomes as we suspect both are substrates of autophagic mRNA decay, but this was not the result. First, *COX5A* MS2-tagged strains had similar localization patterns to the PGK1-MS2 tagged strains as the mRNA was visualized constantly throughout the cytoplasm and did not colocalize with autophagosomes. However, we did observe strong MS2-CP-DsRed signal within the vacuole in some cells. This result could suggest that *COX5A* mRNA or the MS2-coat protein underwent autophagy. DPI8-MS2 tagged mRNA had an odd result because in some cells, it was again localized throughout cytoplasm, however the MS2-CP-DsRed signal in all the *DPI8* strains was very faint, so we cannot conclude its exact localization (Figure 11). These experiments would need to be replicated after the plasmid expressing the fusion dsRed MS2 coat protein is validated as correct.

***PGK1*, *DPI8*, and *COX5A* mRNAs Localization to Stress Granules is Inconclusive**

Finally, we wanted to test to see if we could visualize our three MS2-tagged mRNAs and stress granules, as stress granules undergo autophagy (Buchan et al., 2013), therefore if an mRNA colocalizes with a stress granule, then that mRNA may undergo autophagic mRNA decay through an association with stress granules. To test this, we generated strains that expressed stress granules tagged with the Pab1-GFP marker and the MS2 coat protein fused to mCherry.

First, we unexpectedly observed that stress granules did not appear as circular cytoplasmic foci, but rather appeared to be throughout the cytoplasm. Again, this could be due to a technical error or the stress granules not being correctly tagged with GFP. All three mRNAs tagged with MS2 did not appear to colocalize with stress granules. MS2-tagged *PGK1* and *DPI8* were localized to the cytoplasm, while *COX5A* MS2-tagged mRNA had faint localization to the vacuole again (Figure 12). Since we had used the MS2-CP-dsRed plasmid for these experiments, we cannot conclusively say where the MS2 tagged mRNAs are localized to in these strains.

We were hoping to observe the localization of the *DPI8* and *COX5A* and test if they associated with autophagosomes, stress granules, and mitochondria, but we found the mRNAs localized to different areas of the cell than we expected. Although we were not able to perform our intended experiments, we were able to collect data to determine that our MS2 RNA localization system using MS2-CP-GFP can be successfully used to determine the localization of mRNA in a live cell.

Discussion

First, we sought to understand how Xrn1 and Rny1 work in parallel pathways to create functioning mitochondria during the post-diauxic phase. Using microscopy, we were able to discern Xrn1 and Rny1's localization in the post-diauxic phase. Xrn1 was confirmed to be localized with P-Bodies in the post-diauxic phase. Since P-Bodies contain all of the degradation machinery that Xrn1 would need to degrade mRNA, this suggests that Xrn1 may still function as it normally would in the log phase. This result contradicts the findings from Grousl et al, because Xrn1 was localized to P-Bodies in the post-diauxic phase, whereas they suggested that Xrn1 completely changed its localization to eisosomes at the cell membrane during these conditions. P-Bodies are seen during all growth phases, but increase in number during

conditions of stress, such as the post-diauxic phase. Therefore, we assume that Xrn1 is working to alter the gene expression profile more during these conditions. However, when the cells were grown in ethanol media, we observed that P-Bodies localized to what we suspect is the vacuole, while Xrn1 remained in the cytoplasm. This could indicate that components of P-Bodies underwent autophagy. It has been observed previously that P-Bodies undergo autophagy (Buchan et al., 2013), but more experiments are needed to determine if this is occurring. For example, we will need to tag P-Bodies with one fluorescent protein and vacuoles with another and see if these two components colocalize in media containing ethanol. If colocalization does occur, then we can confirm that P-Bodies do in fact undergo autophagy during ethanol-induced stress.

Previous research performed by Thompson and Parker determined that Rny1 leaves the vacuole during stress and enters the cytoplasm (Thompson et al., 2009). However, the localization of Rny1 during the post-diauxic phase was unclear, and we wanted to observe its localization for ourselves. Our experiments suggest that Rny1 is not detected in the log phase. However, Rny1 localized with mitochondrial-like structures in the cytoplasm during the post-diauxic phase. This corresponds with research previously done with the human analog of Rny1, RNASET2. In these experiments, it was established that RNASET2 localizes within mitochondria in human cells (Liu et al., 2017). This result is in line with our hypothesis that Rny1 may work in a pathway to help promote proper mitochondrial function. If Rny1 truly localizes to mitochondria, then it must function to presumably degrade mRNA that is translated on the surface of the mitochondria. We are currently testing that Rny1 colocalizes with mitochondria by taking our Rny1-GFP strain and transforming in the mitochondrial-mCherry plasmid. We will

use the same experimental conditions as used before to see if Rny1 and mitochondria colocalize in the post-diauxic phase. Finally, in our ethanol experiments, we did not observe Rny1 in the cells due to autofluorescence. This was an unexpected result because we would assume that Rny1 would be detected because the cells were placed under a stressful condition. We will need to replicate this experiment with another brighter, fluorescently-tagged protein to diminish the autofluorescence and see if Rny1 is can be visualized under these conditions.

To test if an autophagic mRNA pathway existed, we sought to optimize the use of the MS2 system to visualize mRNA localization of potential targets of autophagic mRNA decay. Visualization of the various components necessary for the MS2 system and potential markers proved to be problematic. *PGK1* mRNA was used as our control because it was not affected by *rny1Δ* and *atg15Δ*, while *DPI8* and *COX5A* mRNAs levels were increased in these mutants, suggesting that they may be targets for autophagic mRNA decay. We observed that *PGK1* mRNA localized with mitochondria in the post diauxic phase. *DPI8* localized to the cytoplasm in all three strains, however the GFP fluorescence in this strain was not as strong as we anticipated, and therefore we cannot determine if *DPI8* truly localized to the cytoplasm or if the signal we observed was autofluorescence. We cannot explain why this occurred, but we will need to replicate these experiments to determine if an experimental error occurred and if this is in fact what is happening in the cell. Finally, *COX5A* was the most consistent with its localization out of the three mRNAs. In two out of the three strains, we saw *COX5A* localized to the vacuole of the cell in the post-diauxic phase. Though this signal may be an artifact as we expected to see *COX5A* associate with mitochondria, it is tempting to speculate that the mRNA underwent degradation by autophagy because it was found in the vacuole. Another possibility

is that *COX5A* is localized to the nucleus instead of the vacuole. This could be because *COX5A* MS2 tagged mRNA was not exported from the nucleus into the cytoplasm. To confirm where exactly it is localized, we will need to tag the vacuole with one fluorescent protein and the nucleus with another and see what *COX5A* colocalizes with in the post-diauxic phase. Overall, we must replicate all of these experiments to first confirm that our MS2 tagging technique is working correctly. We observed inconclusive results when using the MS2-CP-DsRed plasmid, and therefore we need to tag our mRNAs with a different marker because we cannot trust any of our results with this plasmid. We can use the pMS2-CP-3xGFP plasmid to tag our mRNAs because we were able to see the expected fluorescence of PGK1 in Figure 10, so we know that this marker for MS2 mRNAs worked correctly.

Once our experimental setup has been optimized, we have the potential to provide evidence that a mRNA autophagic decay pathway exists. Secondly, we hope to test the dependence of the autophagic mRNA decay pathway on the ribonucleases by making *rny1Δ*, and an *xrn1Δ* in our MS2-tagged *PGK1*, *DPI8*, and *COX5A* strains. Then, we will transform the plasmids that contain the tagged autophagosomes, stress granules, and mitochondria, and visualize the cells in the post-diauxic phase. We are hoping that this will shed some light on how Xrn1 and Rny1 influences these mRNA levels in the post-diauxic phase through understanding how the mRNA substrates interact with different structures that maybe involved in autophagic mRNA decay in the cell.

Overall, we were able to determine the localization of certain mRNAs in a live cell during the post-diauxic phase using the MS2-GFP protein, while we are skeptical of the MS2-DsRed protein. We have determined that Xrn1 may have a very important role in mRNA decay, and its

localization in the post-diauxic phase (localizes with P-Bodies) does not suggest that Xrn1 changes its function during stress. On the other hand, we believe that Rny1 localizes to mitochondria in the post-diauxic phase, but more experiments are needed to confirm this result.

Overall, how the cell quickly adapts to post-diauxic phase using mRNA decay is an understudied topic and can provide insight to how mRNA decay promotes homeostasis. Though studying gene expression and mRNA decay can give insight on how *S. cerevisiae* functions, it also has been determined that many of these processes have connections with neurodegenerative diseases. Specifically, mutations in processes related to mRNA stability and decay have been found to trigger cell toxicity leading to degenerative diseases such as Amyotrophic Lateral Sclerosis (ALS), Frontotemporal Lobar Degeneration (FTLD), Fragile X Syndrome, and many others (Buchan et al., 2013; Ramaswami et al., 2013). Therefore, if we can understand the mechanism and functions of mRNA decay in *S. cerevisiae*, then it could help to understand the pathogenesis of these diseases in humans. On the other hand, there are many neurodegenerative diseases that come as a result of mitochondrial dysfunction. Alzheimer's disease (AD), Parkinson's disease (PD), Amyotrophic Lateral Sclerosis (ALS), and Huntington's disease, (HD) just to name a few (Lin et al., 2006). Most of these neurodegenerative diseases are due to an accumulation or mutations within the mitochondrial DNA (mtDNA) that occur during aging. As these specific mutations accumulate, it has the potential to cause mitochondrial dysfunction, thus leading to these neurodegenerative diseases. Aging is an inevitable process, however, if we can understand the mechanisms that lead to mitochondrial

dysfunction, then we could better fight these neurodegenerative diseases that impact so many lives.

Materials and Methods

Yeast Strains and Media

Saccharomyces cerevisiae strains in this study were BY4741. Yeast cultures were grown in liquid YPAD media (2% yeast extract, 4% peptone, 0.0048% Adenine Hemisulfate, 2% glucose) or liquid SC media (3.4% YNB without amino acids and ammonium sulfate, 10% Ammonium Sulfate, 5% glucose, supplemented with a complete or appropriate mixture of amino acids) with shaking at 30°C. Cells were grown for 3.5 hours to be visualized in the log phase, and 20 hours for post-diauxic phase. Solid media that corresponded with each given strain contained 2% (w/v) agar. To select for plasmids, either the specific amino acid was left out of the media or the corresponding antibiotic was added to the media to select for resistance to geneticin. Ethanol media was made with the normal YPAD recipe with 3% ethanol added instead of glucose.

Microscopy

For MS2 imaging, the cells were grown overnight in selective SC media, back-diluted, and grown to specific time periods. For time periods, the cells were grown overnight and back-diluted to an $(OD_{600}) = 0.2$ 12 hours after inoculation in fresh SC media and imaged 5, 24, and 30 hours. The cells were then centrifuged and placed on a glass slide with a slice of 1.5% agarose in selective media.

Confocal live cell imaging was performed using a confocal microscope with a 100x lens oil-immersion objective. Fluorescence signals of GFP and mRFP (see table 2 for exposure conditions). The images were processed using FIJI ImageJ software.

Construction of Strains

The MS2 strains were constructed first by PCR amplification of B29 (see table 1) with homology arms (50nt) from the mRNA genes of interest (PGK1, DPI8, and Cox5a). This cassette was then transformed into the WT BY4741 strain. Kanamycin resistance was used to confirm the cassette and was transformed correctly along with the Zymolase colony PCR. The kanamycin resistance gene was then removed by inducing the *GAL1* promoter with galactose to express CRE recombinase to remove the marker. Each isolate that did not grow on kanamycin resistance plates were then patched from a YPAD plate onto plates containing 5-FOA or G418. These were used to confirm the kanamycin resistance gene and CRE recombinase plasmid were both removed. Finally, plasmids expressing GFP and mRFP were transformed into each cell line and were confirmed using amino acid selection.

For Xrn1 and Rny1 strains, GFP and mCherry plasmids were transformed in and confirmed with Kanamycin resistance drugs. For Xrn1 and Rny1 deletion strains, a PCR was performed with primers containing homology arms (50nt) from the genes of interest (Xrn1 or Rny1) and amplified the Kanamycin gene. The PCR product was transformed into the WT BY4741 strain and Kanamycin resistance was used to confirm the PCR product was present. Zymolase colony PCRs were then used to confirm the PCR product was inserted in the correct position. 1% agarose gels were used for gel electrophoresis.

Table 1: Plasmids

Plasmid ID	Plasmid (Yeast Selection)
B20	Pedc3-mCH (URA+)
B29	pET264-p415 24xMS2V6 (KanR)
B33	pSH47 (KanR)
B39	pMS2-CP 2xdsRed 3.1 (HIS+)
B40	pPab1-GFP (LEU+)
B41	pGFP-Atg8 (415) (LEU+)
B42	pMito-Dsred (URA+)
B43	pMS2-CP-3xGFP (HIS+)

Table 2: Exposure Conditions

Strain	Exposure Time GFP	Exposure Time mCherry
PGK1+ATG8	0.25	1.00
DPI8+ATG8	0.10	1.00
Cox5a+ATG8	0.10	1.00
PGK1+Pab1	0.1	1.00
DPI8+Pab1	0.01	1.00
Cox5a+Pab1	0.01	1.00
PGK1+Mito	0.25	0.025
DPI8+Mito	0.25	1.00
Cox5a+Mito	0.25	1.00

Xrn1	0.10	0.25
Rny1	0.25	1.99

Table 3: Primers

Primer ID	5'-3- Sequence
CC29	CTTCACCTTCTCCACTGACAG
CC30	AAAAATCAACACTTGTAACAACAGCAGCAACAAATATATATCAGTACGGTGGATCCCCGG
CC31	GATATACTATTAAGTAACCTCGAATATACTTCGTTTTAGTCGTATGTTTGGATCTGATATCATCGATGAATTCG
CC32	GGACGATTCGTGTACTATAAGGAG
CC33	GCTACACCCTACAGGAGGATTATTG
CC34	CCAGCACCTGAGAACAGGTTTGC
CC43	TGGAAGGTAAGGAATTGCCAGGTGTTGCTTTCTTATCCGAAAAGAAATACCGCTCTATAGAAC TAGTGGAT
CC44	GGAAAGAGAAAAGAAAAAATTGATCTATCGATTTCAATTCAATTCAATTGCATAGGCCACTA GTGGATCTG
CC45	GGCTTCAAGCTTACACAACACGG
CC46	GTGCCTCACTAGCTACCAGAAGACACTTGGCTCACGCGCCAAAGTTGTAGCCGCTCTAGAACT AGTGGAT
CC47	GTCATCATCATTAAATAAACCAGGAAAGAAAAGAGCATAATTAAGATACGCGCATAGGCCACTA GTGGATCTG
CC48	GTGCAAGCAAGTACGAATGTCC
CC49	CGAAGAATGCTAATCCTTGGGGTGGTTATTCTCAGGTCCAATCTAAATGACCGCTCTAGAACTA GTGGAT
CC50	CATGACAATCGTTAACCCCTATTGATTTCTTTCAAATTTCTGGCCTGTGCATAGGCCACTAGT GGATCTG
CC51	GGCGGATGCCCATGGATACAC
CC52	GCCATCCTATGGAACTGCCTC
CC66	GTAAATATGTAATAAAAATTAAGATGGGCAGACATTTATCATTTTGCTTACGGATCCCCGGGT TAATTAA
CC67	GGCTTGGCTTTAAGCTCTAATTCCGTCTGCATTCGTAATAGAAATATCTCGAATTCGAGCTCGTT TAAAC
CC68	GAGCGGGATATGGAAAGAGTGGG
CC69	CAACGCCAAGAACCGTGTCTCG
CC70	GAGCAGGAGAAAGTCATATGGCG
CC71	GATGACCAAGACTTTGATGGTG

CC98 F	GCCACATGGTGGTTATGTAGCAAAG
CC98 R	CCAATCAATATCCCTTCCTTCCTC
JG1	TTGTTCTATTTTAATCAAATGTTAGCG
JG2	GCACGTCAAGACTGTCAAGG
JG9	CCTACATATCAATGCATTCAAC
JG10	GCCAGATAATTGTCATGGTG
JG11	CGTGTATCCATAAGGACTCATG
JG12 1	CTATTGCAAGGCCAACTATTTAAGATATTTCAAACAAAGTACTGTGTACGGATCCCCGGGTT AATTAA
JG12 2	TTTCTTCTCAGAGAAGGGTAAAGCTAAATGAAGTTTTCAATCGGAAAACCTGAATTCGAGCTC GTTTAAAC
JG13 9	GTACTTACGACTTCCAATTACCG
JG14 0	GATAACTTATACCTGGATATGAATTCG
JG14 1	TGAATCTACGAGCTCTTTGTTG
JG18 2	GACTAGCTCACCAGTAAGAACTG
JG23 3	CGAATGGAGCAGATAAGGGTATAGAACCAAACCTGCCCTATAAACATTCCATTATCCGGATCCC CGGGTTAATTAA
JG23 4	CAAGTGGTTATAATACCATACTTCGTTTAAGGAATTATGTCTATCACAGCCTGAATTCGAGCTC GTTTTCGACAC
JG24 9	TTCTTCTCAGAGAAGGGTAAAGCTAAATGAAGTTTTCAATCGGAAAACCTGGATCTGATATCAT CGATGAATTCG
JG28 9	TAGTAAAAAAGTGAGTAGGAACGTGTATGTTTGTGTATATTGGAAAAAGGGGATCTGATATCA TCGATGAATTCG
JG29 0	TGAAGTCCTAATCACAAAAGCAAAAAAATCTGCCAGGAACAGTAAACATGGATCCCCGGGTT AATTAA
JG29 9	GGTGCAGTAAGCTTCCTGAGG
JG30 0	GTTGCCGGATATGTCAATGGAC
JG30 1	CCTCATCTAAAAGCATGCCACC

Table 4: Yeast Strains

Strain Number	Genotype
SC19	WT + EDC3-mCherry plasmid
SC21	Xrn1-GFP
SC22	PAG32 <i>xrn1Δ::HPHMx</i>
SC24	C-terminal GFP tag on Rny1
SC26	Xrn1-GFP + EDC3-mCherry plasmid
SC28	Rny1-GFP (internal tag)
SC29	<i>rny1Δ::KanMx</i>
SC30	<i>PGK1</i> +MS2 cassette
SC33	<i>DPI8</i> +MS2 cassette
SC37	<i>COX5A</i> +MS2 cassette
SC43	<i>rny1Δ::KanMx</i>
SC71	<i>PGK1</i> with pPGFP-Atg8 and MS2-CP 1xdsRed
SC73	<i>DPI8</i> with pPGFP-Atg8 and MS2-CP 1xdsRed
SC75	<i>COX5A</i> with pPGFP-Atg8 and MS2-CP 1xdsRed
SC77	<i>PGK1</i> with pPab1-GFP and MS2-CP 1xdsRed
SC79	<i>DPI8</i> with pPab1-GFP and MS2-CP 1xdsRed
SC81	<i>COX5A</i> with pPab1-GFP and MS2-CP 1xdsRed
SC83	<i>PGK1</i> with Mito-DsRed and pMS2-CP-3xGFP
SC85	<i>DPI8</i> with Mito-DsRed and pMS2-CP-3xGFP

SC87	COX5A with Mito-DsRed and pMS2-CP-3xGFP
SC89	PGK1 with MS2-CP 1xdsRed
SC90	DPI8 with MS2-CP 1xdsRed
SC91	COX5A with MS2-CP 1xdsRed
SC92	PGK1 with pMS2-CP-3xGFP
SC93	DPI8 with pMS2-CP-3xGFP
SC94	COX5A with pMS2-CP-3xGFP
SC95	WT with Atg8 and MS2-CP 1xdsRed

Works Cited

1. Tomas Grousl, Miroslava Opekarová, Vendula Stradalova, Jiri Hasek, Jan Malinsky. Evolutionarily conserved 5'-3' exoribonuclease Xrn1 accumulates at plasma membrane-associated eisosomes in post-diauxic yeast. *PLoS One*. 2015;10(3):e0122770. <https://www.ncbi.nlm.nih.gov/pubmed/25811606>. doi: 10.1371/journal.pone.0122770.
2. Alirezaei M, Kemball CC, Flynn CT, Wood MR, Whitton JL, Kiosses WB. Short-term fasting induces profound neuronal autophagy. *Autophagy*. 2010;6(6):702-710. <http://www.tandfonline.com/doi/abs/10.4161/auto.6.6.12376>. doi: 10.4161/auto.6.6.12376.
3. Welter E, Elazar Z. Autophagy mediates nonselective RNA degradation in starving yeast. *The EMBO Journal*. 2015;34(2):131-133. <https://onlinelibrary.wiley.com/doi/abs/10.15252/emj.201490621>. doi: 10.15252/emj.201490621.
4. Peipei Liu;Jinliang Huang;Qian Zheng;Leiming Xie;Xinping Lu;Jie Jin;Geng Wang. Mammalian mitochondrial RNAs are degraded in the mitochondrial intermembrane space by RNASET2. *Protein*

- Cell*. 2017;8(10):735-749. <http://lib.cqvip.com/qk/71234X/201710/673698841.html>. doi: 10.1007/s13238-017-0448-9.
5. Youle RJ, Narendra DP. Mechanisms of mitophagy. *Nature Reviews Molecular Cell Biology*. 2011;12(1):9-14. <http://dx.doi.org/10.1038/nrm3028>. doi: 10.1038/nrm3028.
6. Joseph L. DeRisi, Vishwanath R. Iyer, Patrick O. Brown. Exploring the metabolic and genetic control of gene expression on a genomic scale. *Science*. 1997;278(5338):680-686. <http://www.sciencemag.org/content/278/5338/680.abstract>. doi: 10.1126/science.278.5338.680.
7. Buchan J , Kolaitis R, Taylor J , Parker R. Eukaryotic stress granules are cleared by autophagy and Cdc48/VCP function. *Cell*. 2013;153(7):1461-1474. <https://www.sciencedirect.com/science/article/pii/S0092867413006430>. doi: 10.1016/j.cell.2013.05.037.
8. Takeshi Noda, Yoshinori Ohsumi. Tor, a phosphatidylinositol kinase homologue, controls autophagy in yeast. *Journal of Biological Chemistry*. 1998;273(7):3963-3966. <http://www.jbc.org/content/273/7/3963.abstract>. doi: 10.1074/jbc.273.7.3963.
9. Beal MF, Lin MT. Mitochondrial dysfunction and oxidative stress in neurodegenerative diseases. *Nature*. 2006;443(7113):787-795. <http://dx.doi.org/10.1038/nature05292>. doi: 10.1038/nature05292.
10. Najafpour G, Younesi H, Syahidah Ku Ismail K. Ethanol fermentation in an immobilized cell reactor using *saccharomyces cerevisiae*. *Bioresource Technology*. 2004;92(3):251-260. <https://www.sciencedirect.com/science/article/pii/S0960852403002414>. doi: 10.1016/j.biortech.2003.09.009.
11. Gustavo C. MacIntosh, Pauline A. Bariola, Ed Newbiggin, Pamela J. Green. Characterization of Rny1, the *saccharomyces cerevisiae* member of the T2 RNase family of RNases: Unexpected

functions for ancient enzymes? *Proceedings of the National Academy of Sciences of the United States of America*. 2001;98(3):1018-1023. <http://www.pnas.org/content/98/3/1018.abstract>.

12. Klionsky DJ, Emr SD. Autophagy as a regulated pathway of cellular degradation. . 2000. https://www.openaire.eu/search/publication?articleId=od_____267::a7b37ab7d6f5e13423cf7ab64ca22732.

13. Tutucci E, Vera M, Biswas J, Garcia J, Parker R, Singer RH. An improved MS2 system for accurate reporting of the mRNA life cycle. *Nature methods*. 2018;15(1):81-89. <https://www.ncbi.nlm.nih.gov/pubmed/29131164>. doi: 10.1038/nmeth.4502.

14. Andrea A Duina, Mary E Miller, Jill B Keeney. Budding yeast for budding geneticists: A primer on the *Saccharomyces cerevisiae* model system. *Genetics*. 2014;197(1):33. <https://search.proquest.com/docview/1530420417>. doi: 10.1534/genetics.114.163188.

15. Stahl G, Salem SNB, Chen L, Zhao B, Farabaugh PJ. Translational accuracy during exponential, postdiauxic, and stationary growth phases in *Saccharomyces cerevisiae*. *Eukaryotic Cell*. 2004;3(2):331-338. doi: 10.1128/EC.3.2.331-338.2004.

16. Zemirli N, Morel E, Molino D. Mitochondrial dynamics in basal and stressful conditions. *International journal of molecular sciences*. 2018;19(2):564. <https://www.ncbi.nlm.nih.gov/pubmed/29438347>. doi: 10.3390/ijms19020564.

17. Natalie Luhtala, Roy Parker. Structure-function analysis of Rny1 in tRNA cleavage and growth inhibition. *PLoS One*. 2012;7(7):e41111. <https://search.proquest.com/docview/1326223666>. doi: 10.1371/journal.pone.0041111.

18. Debrah M. Thompson, Roy Parker. The RNase Rny1p cleaves tRNAs and promotes cell death during oxidative stress in *saccharomyces cerevisiae*. *The Journal of Cell Biology*. 2009;185(1):43-50. <https://www.jstor.org/stable/20537227>. doi: 10.1083/jcb.200811119.
19. Huang H, Kawamata T, Horie T, et al. Bulk RNA degradation by nitrogen starvation-induced autophagy in yeast. *The EMBO Journal*. 2015;34(2):154-168. <https://onlinelibrary.wiley.com/doi/abs/10.15252/emboj.201489083>. doi: 10.15252/emboj.201489083.
20. Joseph L. DeRisi, Vishwanath R. Iyer, Patrick O. Brown. Exploring the metabolic and genetic control of gene expression on a genomic scale. *Science*. 1997;278(5338):680-686. <http://www.sciencemag.org/content/278/5338/680.abstract>. doi: 10.1126/science.278.5338.680.
21. Scientific report. *Scientific report*.
22. Luis J. García-Rodríguez, Anna Card Gay, Liza A. Pon. Puf3p, a pumilio family RNA binding protein, localizes to mitochondria and regulates mitochondrial biogenesis and motility in budding yeast. *The Journal of Cell Biology*. 2007;176(2):197-207. <https://www.jstor.org/stable/30049757>. doi: 10.1083/jcb.200606054.
23. Eduardo Cebollero, Fulvio Reggiori, Claudine Kraft. Reticulophagy and ribophagy: Regulated degradation of protein production factories. *International journal of cell biology*. 2012;2012:182834-9. <http://dx.doi.org/10.1155/2012/182834>. doi: 10.1155/2012/182834.
24. Houseley J, Tollervey D. The many pathways of RNA degradation. *Cell*. 2009;136(4):763-776. <https://www.sciencedirect.com/science/article/pii/S0092867409000671>. doi: 10.1016/j.cell.2009.01.019.
25. Vasicova P, Lejskova R, Malcova I, Hasek J. The stationary-phase cells of *saccharomyces cerevisiae* display dynamic actin filaments required for processes extending chronological life

span. *Molecular and cellular biology*. 2015;35(22):3892-

3908. <https://www.ncbi.nlm.nih.gov/pubmed/26351139>. doi: 10.1128/MCB.00811-15.

26. Luciano Galdieri, Swati Mehrotra, Sean Yu, Ales Vancura. Transcriptional regulation in yeast during diauxic shift and stationary phase. *OmicS : a journal of integrative biology*. 2010;14(6):629-

638. https://www.openaire.eu/search/publication?articleId=od_____267::5f3df9170f443c6804016f4c74a77179. doi: 10.1089/omi.2010.0069.

27. Ramaswami M, Taylor J , Parker R. Altered ribostasis: RNA-protein granules in degenerative disorders. *Cell*. 2013;154(4):727-

736. <https://www.sciencedirect.com/science/article/pii/S009286741300946X>. doi: 10.1016/j.cell.2013.07.038.

28. Chapter1FMBE J. Effects of non-thermal microwave exposures on the proliferation rate of *saccharomyces cerevisiae* yeast. . . doi: 10.1007/978-3-642-29305-4_14.

29. Wang W, Nishikawa T, Isono K. Isolation and characterization of *saccharomyces cerevisiae* genes differentially expressed under different growth conditions. *The Journal of General and Applied Microbiology*. 1997;43(4):217-224. <https://jlc.jst.go.jp/DN/JALC/00084347640?from=SUMMON>. doi: 10.2323/jgam.43.217.